JACS
JOURNAL OF THE AMERICAN CHEMICAL SOCIETY

COMMUNICATION

pubs.acs.org/JACS

Selective Extraction of Large-Diameter Single-Wall Carbon Nanotubes with Specific Chiral Indices by Poly(9,9-dioctylfluorene-*alt*-benzothiadiazole)

Masayoshi Tange,* Toshiya Okazaki,* and Sumio Iijima

Nanotube Research Center, National Institute of Advanced Industrial Science and Technology (AIST), Tsukuba 305-8565, Japan

Supporting Information

ABSTRACT: Semiconducting single-wall carbon nanotubes (SWCNTs) having large diameters (d_t > 1.3 nm) are successfully extracted in toluene by fluorene-based polymers. In particular, poly(9,9-dioctylfluorene-*alt*-benzothiadiazole) shows excellent selectivity for (15,4) SWCNTs. Although the importance of structural matching between the fluorene backbone and the tube surface has already been discussed, the present photoluminescence studies reveal that matching the energy levels between fluorene-based polymers and SWCNTs is crucial for selective nanotube extractions.

One striking feature of single-wall carbon nanotubes (SWCNTs) is that they show metallic or semiconducting properties, depending on the tube diameter (d_t) and the wrapping angle (θ). The extraction technique is therefore highly important for various applications of SWCNTs, such as electronics and photonics. For example, making a field-effect transistor from pure semiconducting SWCNTs with specific structures effectively improves its device performance.[1] Fluorene-based polymers such as poly(9,9-di-*n*-octylfluorene) (PFO) are π-conjugated polymers that have attracted intense interest not only as organic light-emitting polymers with high fluorescence quantum yield and charge mobility[2] but also as dispersing agents for semiconducting SWCNTs in organic solvents.[3,4] Ultracentrifugation of the produced dispersions can lead to selective extraction of specific (n,m) SWCNTs, which is known as the polymer-wrapping technique.[3−6] The rigidity of the polymer backbone is important for interacting with the surfaces of specific semiconducting SWCNT species through π-staking.[3,4,7] This is consistent with the fact that planarization of the fluorene backbone (i.e., a β-phase formation) can be observed when poor solvents for the fluorene-based polymer are used.[8]

It has already been reported that the polymer-wrapping extraction technique is effective for SWCNTs of <1.2 nm diameter. The largest reported tube diameters of extracted semiconducting SWCNTs are d_t = 1.17 nm for PFO ((9,8) tubes) and d_t = 1.20 nm for poly(9,9-dioctylfluorene-*alt*-benzothiadiazole) (F8BT) ((12,5) tubes).[3,4] However, selective extraction of large-diameter SWCNTs (>1.2 nm) by the polymer-wrapping technique has not yet been achieved. Such large-diameter SWCNTs are important for optical communication in the near-infrared region. For example, SWCNTs samples enriched with (10,9), (12,7), (16,2), and (17,0) tubes are highly desirable for telecommunication applications specifically targeted at 1550 nm.[9] Furthermore, the synthesis of low-dimensional nanostructures with functional molecules inside SWCNTs (such as fluorescent coronene encapsulated into SWCNTs) also requires SWCNTs with large-diameter tubes (d_t > ∼1.3 nm).[10]

The detailed mechanism for selective extraction by the polymer-wrapping technique has not yet been clarified. Even though the rigidity of the fluorene moiety is found to be important, the tube diameter dependence of the extraction cannot be explained by a rule. It is therefore necessary to find other clues for the molecular design of the polymer structure.

Here we report the successful extraction of larger-diameter semiconducting SWCNTs (d_t > 1.3 nm) by using two fluorene-based polymers, poly(9,9-di-*n*-dodecylfluorene) (PFD) and F8BT. In particular, F8BT discriminates the wrapping structures of large-diameter SWCNTs, leading to excellent selection for (15,4) tubes. Detailed spectroscopic analyses reveal that matching of the energy levels of the SWCNTs and the polymer is essential for a strong interaction between F8BT and specific SWCNTs, which results in the "chirality"-selective extraction of SWCNTs.

Figure 1 shows optical absorption spectra of PFD- and F8BT-wrapped SWCNT solutions, together with the reference spectrum of the SWCNTs dispersed in D_2O with sodium dodecyl benzenesulfonate (SDBS). The large-diameter SWCNTs (d_t = 1.2−1.6 nm) normally exhibit three absorption bands at wavelengths of <600, 600−820, and 820−1180 nm that are attributable to the third (S3) interband transition of semiconducting tubes, the first (M1) interband transition of metallic tubes, and the second (S2) interband transition, respectively. These three bands are clearly observed in the absorption spectrum of SDBS-dispersed SWCNTs (Figure 1, black line). On the other hand, the M_1 absorption band is missing in both PFD- and F8BT-wrapped SWCNTs (Figure 1, red and blue lines, respectively). The absence of M1 absorption indicates that semiconducting large-diameter tubes are preferentially extracted from the bulk sample by both polymers. The broad spectral shape of the S2 absorption band of the PFD-wrapped SWCNTs is very similar to that of SDBS-dispersed SWCNTs, suggesting that PFD does not have the selectivity to disperse large-diameter semiconducting tubes with specific chiral indices. In contrast, the S2 absorption band in F8BT-wrapped SWCNTs is obviously structural as compared with those of the PFD-wrapped SWCNTs and the SDBS-dispersed SWCNTs. The structural absorption band

Received: May 23, 2011
Published: July 06, 2011

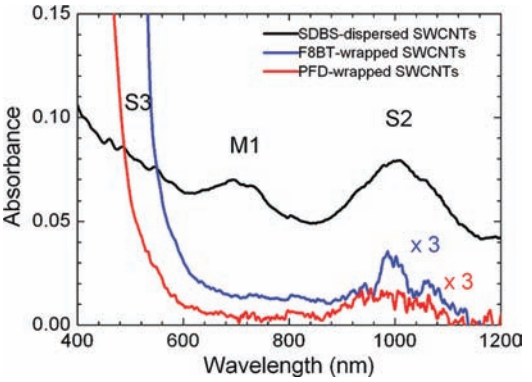

Figure 1. Absorption spectra of SDBS-dispersed SWCNTs in D_2O and F8BT- and PFD-wrapped SWCNTs in toluene. Absorption bands indicated by S3, S2, and M1 are attributed to the third and second interband transitions of semiconducting tubes and the first interband transition of metallic tubes, respectively.

implies that semiconducting tubes with specific chiral indices were extracted by F8BT. Note that the intense signals of the polymer-wrapped SWCNT solutions at the lower wavelengths (<~600 nm) mainly originate from absorptions of PFD and F8BT.

The absorbance of the S2 absorption band in the optical absorption spectrum of the F8BT-wrapped SWCNT solutions is about 0.01. This value is about one-third that of PFO-wrapped HiPco tubes (smaller-diameter tubes).[1] It is known that solubilization of larger-diameter tubes is rather difficult in comparison with that of smaller-diameter tubes. This is probably due to the somewhat stronger van der Waals interactions between the less stiff tubes than between small-diameter tubes.[11]

Figure 2 shows the photoluminescence excitation (PLE) maps of PFD- and F8BT-wrapped SWCNTs in toluene. The PL peaks on the map are clearly seen in the S2 excitation region (λ_{22} = 850−1050 nm) and the S1 emission region (λ_{11} = 1400−1900 nm) of SWCNTs with 1.2−1.6 nm diameter. Each emission peak in the maps can be assigned to specific semiconducting (n,m) SWCNTs on the basis of geometrical patterns observed for carbon nanotube families in a PLE map.[12] Even though the PLE maps appear to show a slightly different pattern for SDBS-dispersed SWCNTs because of the strong absorption of toluene around 1676 nm, the number of PL peaks observed for the PFD-wrapped SWCNTs (Figure 2a) is almost same as that for the SDBS solution.[12] This indicates the interactions between PFD and semiconducting SWCNTs are nearly independent of nanotube structure, which is consistent with the broad absorption spectrum of PFD-wrapped SWCNTs (Figure 1). It is known that PFO exhibits selective dispersion of small-diameter semiconducting tubes (<1.2 nm).[3,4] Despite having the same backbone structure, PFD disperses large-diameter semiconducting tubes with various structures. The different dispersant ability may be associated with the longer alkyl chain of PFD compared to that of PFO. In fact, PFD also disperses small-diameter SWCNTs as well as large-diameter tubes. The high solubility of PFD-wrapped SWCNTs in toluene is consistent with the tendency that the solubility of PFD in organic solvent is higher than that of PFO because of the change in the length of alkyl side chains.[13]

On the other hand, as shown in Figure 2b, F8BT-wrapped SWCNTs exhibit near-infrared emissions from only nine species of semiconducting tubes. In particular, (15,4) semiconducting tubes are preferentially extracted, for which the diameter is 1.38 nm (also see inset of Figure 4). The value of 1.38 nm is much larger than the largest limit reported so far obtained by the polymer-wrapping techniques ($d_t \approx 1.2$ nm).[3−6] Although F8BT is a well-known dispersing agent for specific small-diameter SWCNTs,[3,4] the present result clearly indicates that large-diameter semiconducting tubes are also selectively extracted by the polymer.

To investigate the different dispersant abilities between PFD and F8BT in detail, PLE measurements with excitation at ultraviolet−visible wavelengths were also carried out (Figure 3). The characteristic emissions were observed at ~1280 nm in both PFD- and F8BT-wrapped SWCNT solutions under irradiation of 415 and 510 nm, respectively. The wavelengths of 415 and 510 nm coincide with the onset of absorption bands of each polymer (Supporting Information, Figure S1). It has been reported that PFO and other rigid polymers show absorption peaks at the onset of the original absorption bands that can be explained by formation of excimers or aggregation due to the interpolymer interactions between planar backbones of polymers[8,14] (also see Supporting Information). The emissions around 1280 nm observed here suggest that excimers were formed through the strong interactions between planar polymer backbones in both solutions under the present experimental conditions.

In the higher emission wavelength range (>1480 nm) of Figure 3, the PLE maps show a significant discrepancy between PFD- and F8BT-wrapped SWCNTs. The open circles in

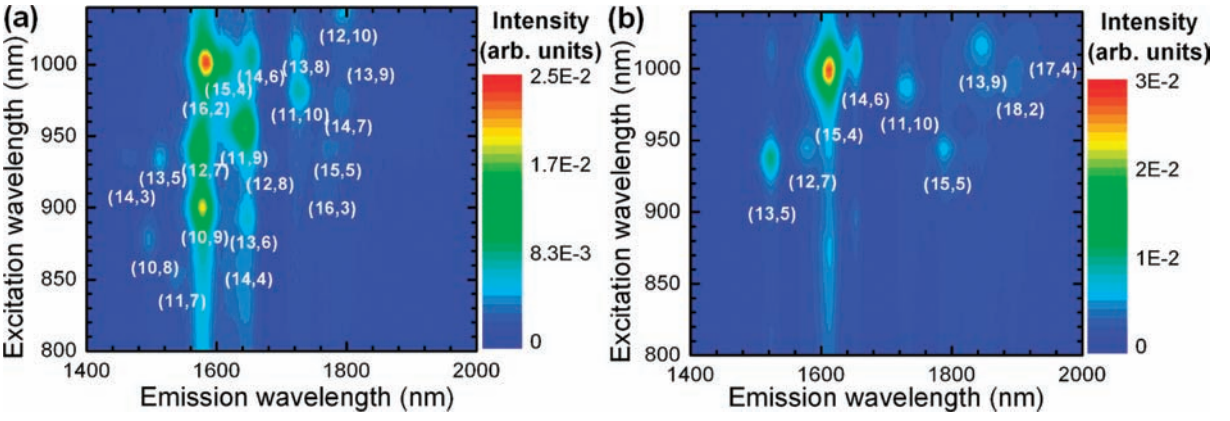

Figure 2. PLE maps excited at near-infrared wavelengths for (a) PFD-wrapped and (b) F8BT-wrapped SWCNTs in toluene. Chiral indices (n,m) of the SWCNTs corresponding to each emission peak are shown.

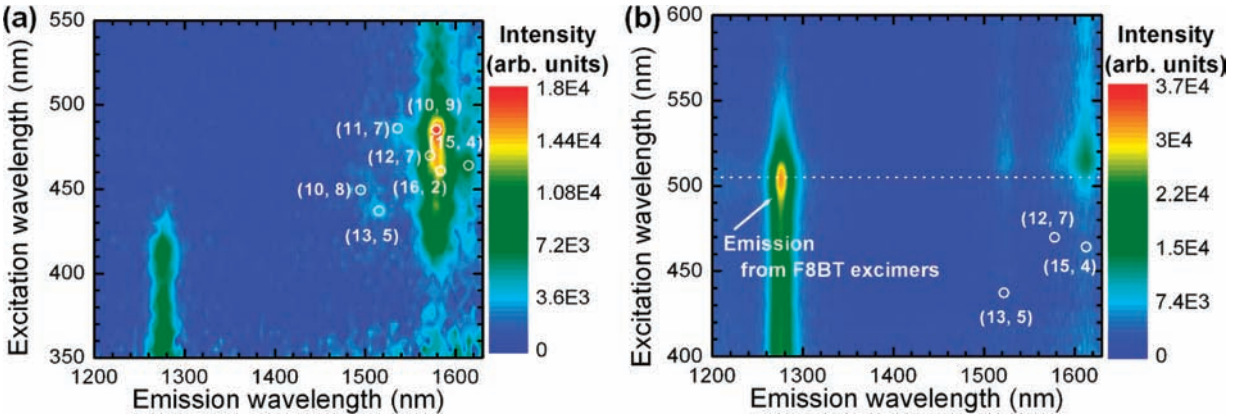

Figure 3. PLE maps excited at UV−vis wavelengths for (a) PFD- and (b) F8BT-wrapped SWCNT solutions. Emission peaks of SWCNTs excited at S3 optical transition wavelengths are indicated by open circles.

Figure 3a denote the observed emission peaks of PFD-wrapped SWCNTs in toluene that are assignable to specific (n,m) semiconducting tubes excited at S3 optical transition wavelengths.[15−17] On the other hand, F8BT-wrapped SWCNTs do not show such emissions through S3 excitations (Figure 3b). Indeed, there are no PL peaks for F8BT-wrapped SWCNTs at the same wavelengths as those of PFD-wrapped SWCNTs (open circles).

Instead, in the PLE map for F8BT-wrapped SWCNTs, intense emissions appear at ∼515 nm excitation (Figure 3b), which is close to the absorption band of the excimer of F8BT, as described above. The similarity reminds us of the energy transfer from excited F8BT to SWCNTs.[18] However, the precise excitation wavelength of the PL peaks is unambiguously longer (515 nm) than that of the F8BT excimers (508 nm, Figure 3b). The apparent red-shift suggests that the emission is due not to energy transfer from F8BT excimers to SWCNTs[18] but to exciplex formation through the interaction between the planar backbone of polymers and the surface of specific SWCNTs. Fluorene-based polymers such as F8BT and PFO are known as charge transport materials (CTMs).[19] Such CTMs can form exciplexes between other light-emitting materials as well as CTMs themselves (excimers).[20,21] The ability of fluorene-based polymers to extract specific SWCNTs seems to be associated with exciplex formation between the polymers and SWCNTs.

For stable exciplex formation, it is important that the energy levels of the polymers are close to those of the counterpart.[20] Normally, the introduction of benzothiadiazole units to the fluorene moiety reduces the lowest unoccupied molecular orbital (LUMO) energy levels, while the highest occupied molecular orbital (HOMO) energy levels remain unaffected.[22] In fact, the electron affinity (E_a, LUMO level) of F8BT (3.2 eV) is considerably larger than that of the corresponding homopolymer PFO (2.6 eV), while the ionization potentials (I_p, HOMO levels) are very similar for the two polymers (5.9 eV for F8BT and 5.8 eV for PFO).[19,23] Figure 4 shows LUMO and HOMO levels of F8BT and PFO (fluorene homopolymer). Unfortunately, to our knowledge, the E_a and I_p of PFD have not been reported. However, it is reasonable to assume that PFD has almost the same E_a and I_p as PFO because the length of the side chain does not significantly affect the HOMO and LUMO levels.[24] Indeed, the onset of the absorption band of PFD is almost identical to that of PFO, which supports this assumption (Figure S1).

The energy levels associating with third van Hove singularities of semiconducting SWCNTs are depicted as open circles in

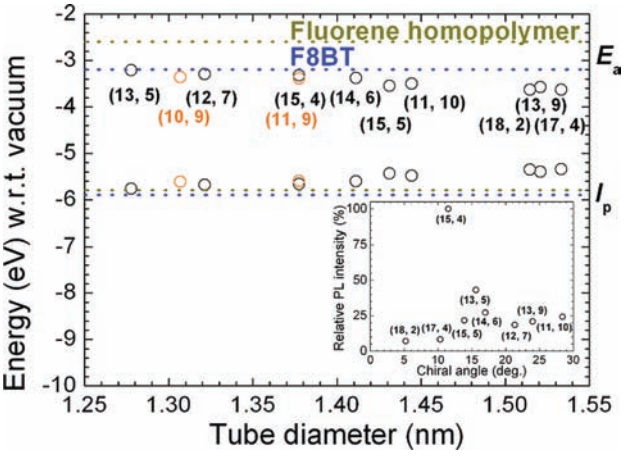

Figure 4. Ionization potential (I_p) and electron affinity (E_a) levels (HOMO and LUMO) of F8BT and fluorene homopolymer (PFO) with third van Hove singularities of near-armchair tubes (orange circles) and of semiconducting SWCNTs extracted by F8BT (black circles). The inset shows PL intensities of F8BT-wrapped SWCNTs relative to (15,4) tubes with chiral angle dependence.

Figure 4,[15] where the work function of the SWCNTs is assumed to be −4.49 eV.[25] Although the energy levels of SWCNTs locate near the HOMO levels of both polymers, the LUMO level of F8BT is much closer to the energy levels of SWCNTs than that of the fluorene homopolymer. This energy level matching may yield stronger interactions between F8BT and SWCNTs than between PFD and SWCNTs, which results in the extraction of specific chiral indices.

Meanwhile, studies of polymer wrapping for small-diameter tubes have shown that F8BT prefers SWCNTs with an intermediate chiral angle ($\theta \approx 19°$), while PFO selectively disperses near-armchair tubes ($\theta \approx 25-28°$).[3,4] The ability of F8BT to extract SWCNTs with smaller chiral angles could be interpreted on the basis of a conformational change of the polymer backbone due to the introduction of co-monomer into fluorene units.[26] Such a conformational change should affect the dispersion selectivity for large-diameter SWCNTs. The inset of Figure 4 shows the relative PL intensity of F8BT-wrapped SWCNTs to the (15,4) tubes as a function of chiral angle θ. Indeed, F8BT seems to enrich specific SWCNTs with intermediate chiral angles (θ = 10−20°). In particular, the PL intensity of (15,4) tubes

($\theta \approx 12°$) is significantly stronger, whereas signals of the near-armchair tubes such as (10,9), (11,9), and (11,10) tubes are missing or severely suppressed. Interestingly, the PL intensity of (15,5) tubes with $\theta \approx 14°$ is low in comparison with those of (15,4) and (13,5) tubes with intermediate chiral angles. This low intensity is consistent with the fact that the upper energy level of (15,5) tubes is lower than that of F8BT (Figure 4). Therefore, the matching of energy levels between fluorene-based polymers and SWCNTs, and structural matching between the fluorene backbone and tube surface, are both important for strong interactions between the polymers and SWCNTs, which leads to the significant difference in selectivity between F8BT- and PFD-wrapped SWCNTs.

In conclusion, we have succeeded in extracting large-diameter SWCNTs using fluorene-based polymers. In particular, F8BT selectively disperses (15,4) SWCNTs with strong interactions, which leads to the formation of a stable exciplex between them. Spectroscopic results obtained here suggest that the energy level matching between SWCNTs and fluorene-based polymers is one of the reasons for selective extraction of SWCNTs having specific chiral indices.

■ ASSOCIATED CONTENT

Supporting Information. Experimental details; optical absorption and excitation spectra of fluorene-based polymers. This material is available free of charge via the Internet at http://pubs.acs.org.

■ AUTHOR INFORMATION

Corresponding Author
masa-tange@aist.go.jp; toshi.okazaki@aist.go.jp

■ ACKNOWLEDGMENT

The authors thank Dr. T. Saito (National Institute of Advanced Industrial Science and Technology) for the experimental help. This work was supported by MEXT KAKENHI (#21685017).

■ REFERENCES

(1) Izard, N.; Kazaoui, S.; Hata, K.; Okazaki, T.; Saito, T.; Iijima, S.; Minami, N. *Appl. Phys. Lett.* **2008**, *92*, 243112.
(2) Neher, D. *Macromol. Rapid Commun.* **2001**, *22*, 1365–1385.
(3) Nish, A.; Hwang, J.-Y.; Doig, J.; Nicholas, R. J. *Nature Nanotechnol.* **2007**, *2*, 640–646.
(4) Chen, F.; Wang, B.; Chen, Y.; Li, L.-J. *Nano Lett.* **2007**, *7*, 3013–3017.
(5) Hwang, J.-Y.; Nish, A.; Doig, J.; Douven, S.; Chen, C.-W.; Chen, L.-C.; Nicholas, R. J. *J. Am. Chem. Soc.* **2008**, *130*, 3543–3553.
(6) Stürzl, N.; Hennrich, F.; Lebedkin, S.; Kappes, M. M. *J. Phys. Chem. C* **2009**, *113*, 14628–14632.
(7) Papadimitrakopoulos, F.; Ju, S.-Y. *Nature* **2007**, *450*, 486–487.
(8) Dias, F. B.; Morgado, J.; Maçanita, A. L.; da Costa, F. P.; Burrows, H. D.; Monkman, A. P. *Macromolecules* **2006**, *39*, 5854–5864.
(9) Hasan, T.; Sun, Z.; Wang, F.; Bonaccorso, F.; Tan, P. H.; Rozhin, A. G.; Ferrari, A. C. *Adv. Mater.* **2009**, *21*, 3874–3899.
(10) Okazaki, T.; Iizumi, Y.; Okubo, S.; Kataura, H.; Liu, Z.; Suenaga, K.; Tahara, Y.; Yudasaka, M.; Okada, S.; Iijima, S. *Angew. Chem., Int. Ed.* **2011**, *50*, 4853–4857.
(11) Tersoff, J.; Ruoff, R. S. *Phys. Rev. Lett.* **1994**, *73*, 676–679.
(12) Okubo, S.; Okazaki, T.; Kishi, N.; Joung, S.-K.; Nakanishi, T.; Okada, S.; Iijima, S. *J. Phys. Chem. C* **2009**, *113*, 571–575.
(13) Teetsov, J.; Fox, M. A. *J. Mater. Chem.* **1999**, *9*, 2117–2122.
(14) Halkyard, C. E.; Rampey, M. E.; Kloppenburg, L.; Stunder-Martinez, S. L.; Bunz, U. H. F. *Macromolecules* **1998**, *31*, 8655–8659.
(15) Araujo, P. T.; Doorn, S. K.; Kilina, S.; Tretiak, S.; Einarsson, E.; Maruyama, S; Chacham, H.; Pimenta, M. A.; Jorio, A. *Phys. Rev. Lett.* **2007**, *98*, 067401.
(16) Haroz, E. H.; Bachilo, S. M.; Weisman, R. B.; Doorn, S. K. *Phys. Rev. B* **2008**, *77*, 125405.
(17) Jia, Y.; Yu, G.; Dong, J. *Nanotechnology* **2009**, *20*, 155708.
(18) Nish, A.; Hwang, J.-Y.; Doig, J.; Nicholas, R. J. *Nanotechnology* **2008**, *19*, 095603.
(19) Campbell, A. J.; Bradley, D. D. C.; Antoniadis, H. *Appl. Phys. Lett.* **2001**, *79*, 2133–2135.
(20) Matsumoto, N.; Nishiyama, M.; Adachi, C. *J. Phys. Chem. C* **2008**, *112*, 7735–7741.
(21) Jenekhe, S. A.; Osaheni, J. A. *Science* **1994**, *265*, 765–768.
(22) Cornil, J.; Gueli, I.; Dkhissi, A.; Sancho-Garcia, J. C.; Hennebicq, E.; Calbert, J. P.; Lemaur, V.; Beljonne, D.; Brédas, J. L. *J. Chem. Phys.* **2003**, *118*, 6615–6623.
(23) Campbell, A. J.; Bradley, D. D. C.; Antoniadis, H. *J. Appl. Phys.* **2001**, *89*, 3343–3351.
(24) Yu, W.-L.; Pei, J.; Cao, Y.; Huang, W. *J. Appl. Phys.* **2001**, *89*, 2343–2350.
(25) Tanaka, Y.; Hirana, Y.; Niidome, Y.; Kato, K.; Saito, S.; Nakashima, N. *Angew. Chem., Int. Ed.* **2009**, *48*, 7655–7659.
(26) Ozawa, H.; Fujigaya, T.; Niidome, Y.; Hotta, N.; Fujiki, M.; Nakashima, N. *J. Am. Chem. Soc.* **2011**, *133*, 2651–2657.